SUPPLEMENTARY INFORMATION

Swift heavy ion irradiated multi-phase calcium borosilicates: implications to molybdenum partitioning, microstructure, and network topology

Karishma B. Patel[*a], *Sylvain Peuget*[b], *Sophie Schuller*[c], *Clara Grygiel*[d], *Isabelle Monnet*[d], *Ian Farnan*[a]

[a] Department of Earth Sciences, University of Cambridge, Downing Street, Cambridge, CB23EQ, UK

[b] CEA, DEN, DE2D, SEVT, LMPA, Marcoule, F-30207 Bagnols-sur-Cèze, France

[c] CEA, DEN, DE2D, SEVT, LDPV, Marcoule, F-30207 Bagnols-sur-Cèze, France

[d] Normandy University, ENSICAEN, UNICAEN, CEA, CNRS, CIMAP, 14000 Caen, France

S1.0 Additional analysis of pristine sample sets

The main text indicates that as both [B_2O_3] and [MoO_3] increased in the CB and CM series respectively, the general order of MoO_4^{2-} tetrahedra in the amorphous phase also increased, and approached a similar structure to that found for crystalline $CaMoO_4$. The Raman spectra in Figures S1 and S2 provide supporting evidence for these claims. While CB23 and CM2.5 show several MoO_4^{2-} vibrational bands that can also be seen for powellite, especially in phase B, all of these compositions were amorphous according to XRD following synthesis. The sensitivity of XRD in detecting $CaMoO_4$ on the nano or micron scale within this context has been discussed elsewhere [1,2], but it can be assumed that XRD is correct in determining that the synthesized heterogeneous glasses in the CM and CB series are amorphous. Therefore, while the molybdenum environment may take on a crystalline-type $CaMoO_4$ structure, it is predicted that there are a sizeable number of structural defects following synthesis that prevents perfect stacking and orientation, and therefore diffraction.

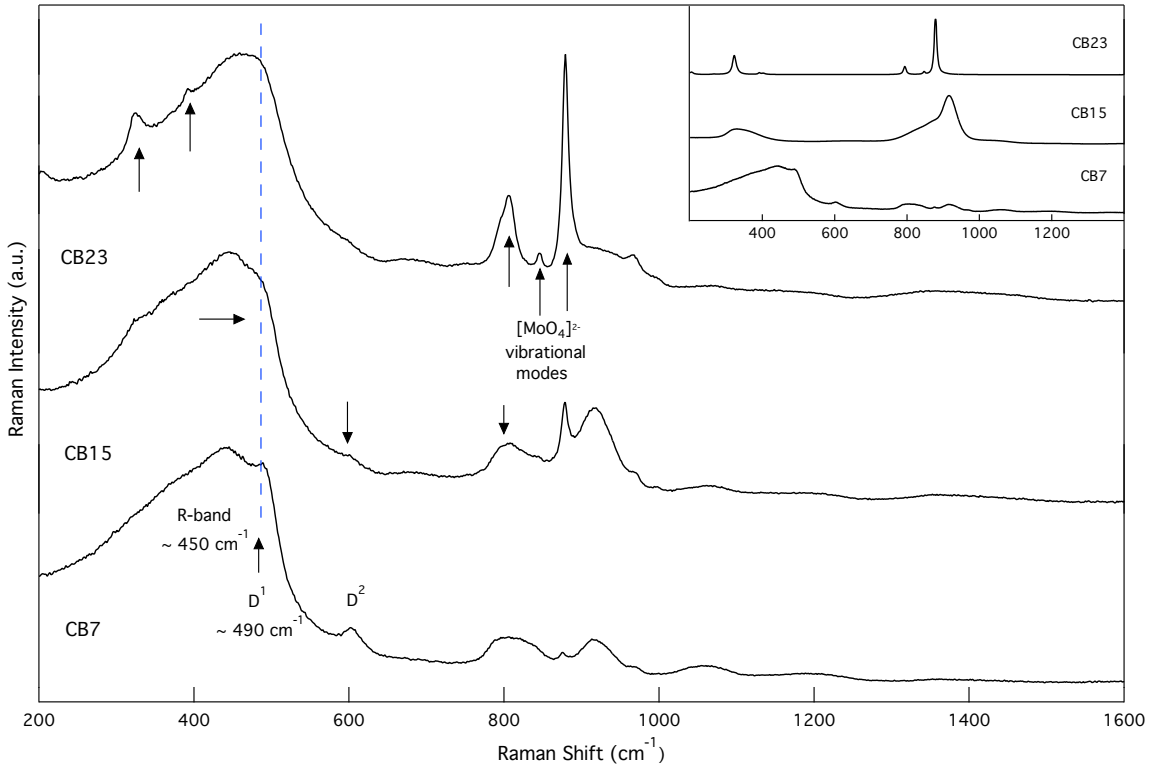

Figure S1. Raman spectra of samples in the CB series with increasing [B_2O_3]. Main spectra represents the Si-rich phase A, while the insert represents CaMo-rich phase B.

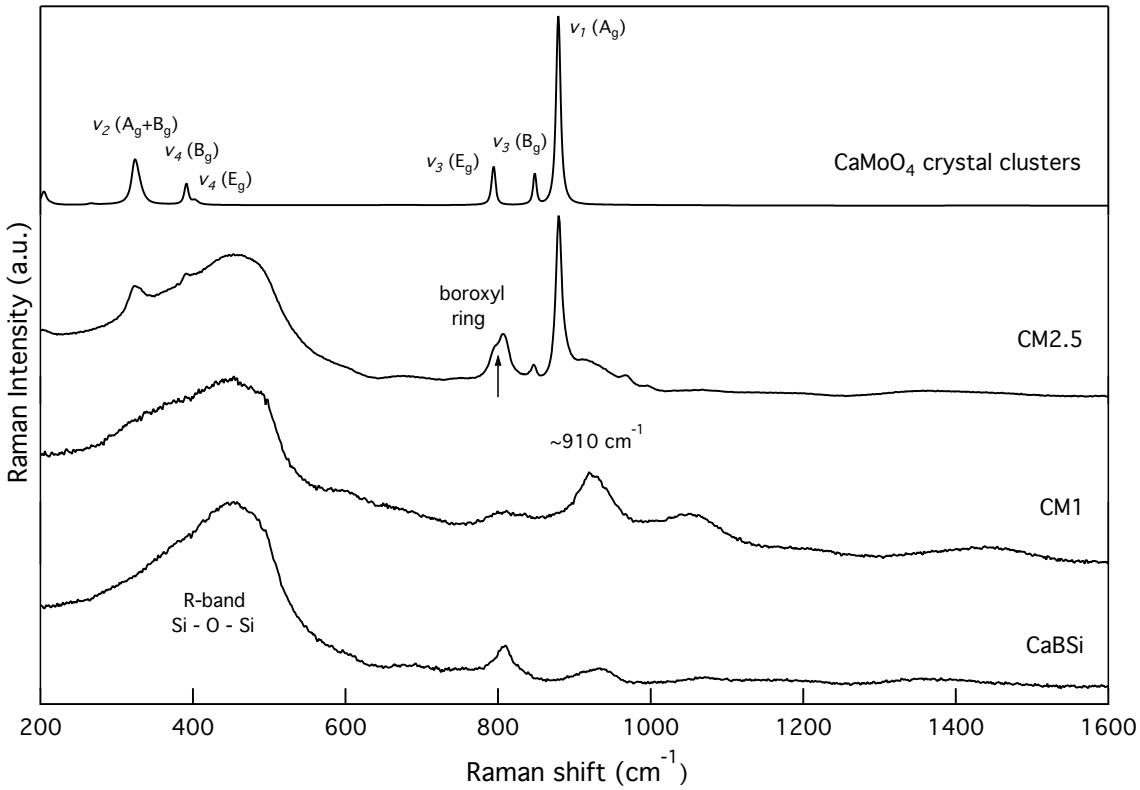

Figure S2. Raman spectra of samples in the CM series with increasing [MoO_3]. An additional spectra for powellite ($CaMoO_4$) crystal clusters in a calcium borosilicate glass is also provided for comparison.

(1) Patel, K. B.; Boizot, B.; Facq, S. P.; Lampronti, G. I.; Peuget, S.; Schuller, S.; Farnan, I. β-Irradiation Effects on the Formation and Stability of CaMoO4 in a Soda Lime Borosilicate Glass Ceramic for Nuclear Waste Storage. *Inorg. Chem.* **2017**, *56*, 1558–1573. https://doi.org/10.1021/acs.inorgchem.6b02657.

(2) Patel, K. B.; Boizot, B.; Facq, S. P.; Peuget, S.; Schuller, S.; Farnan, I. Impacts of Composition and Beta Irradiation on Phase Separation in Multiphase Amorphous Calcium Borosilicates. *J. Non. Cryst. Solids* **2017**, *473*, 1–16. https://doi.org/10.1016/j.jnoncrysol.2017.06.018.

S2.0 EDS results for CM series

Based on morphology changes, the paper introduced the idea of mixing between phases B and C when phase C deposits were 1 – 5 μm in diameter (see section 3.22). EDS maps in Figure S3 support this theory with particles in this size range exhibiting less discrete boundaries. In terms of location, phase C deposits also became more uniformly distributed within phase B following irradiation, which indicates diffusion of ions within phase C.

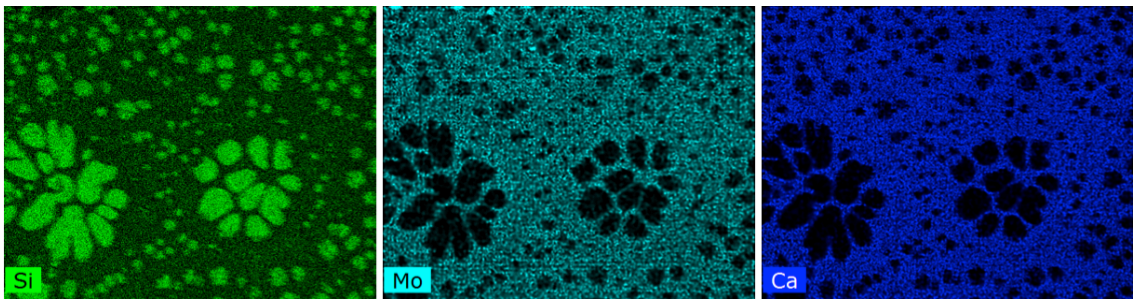

Figure S3. EDS maps of CM2.5 irradiated with 8×10^{13} ions/cm^2 showing increased mixing between phases B and C following irradiation. From left to right: Si (green), Mo (aqua), and Ca (blue). Micrograph dimensions: 150 μm × 110 μm.

It was predicted that the interface between phases was particularly susceptible to irradiation damage owing to the weaker bonds in this region. This would account for the greatest morphological changes being observed in this area, of which diffusion of ions is predicted to play a central role. From analysis across the A – B interface in CM1 (see Figure S4), it is evident that irradiation caused some migration of Ca atoms from phase B to phase A, hence why a decrease in the [Si]/[Ca] ratio was observed in the bulk of phase A, and a decrease of [Ca]/[Mo] was observed in the bulk of phase B. Given the magnitude of change, it is likely that the alteration in [Ca] across the phases was also assisted by an increase in the number of Ca atoms at the surface, and that some Mo entities may have dissolved into the bulk. Nevertheless, the notable decrease in the ratio gradients across the A – B interface does indicate interphase migration of some atoms. The collective results suggest increased disorder and mixing amongst the phases along the A – B interface, with a prominent bulk-to-surface Ca migration. This was similarly found for samples in the CB series, and therefore it suggests a general radiation-

induced mechanism of Ca and Mo diffusion within calcium borosilicate compositions following Xe-irradiation, as described in the main text.

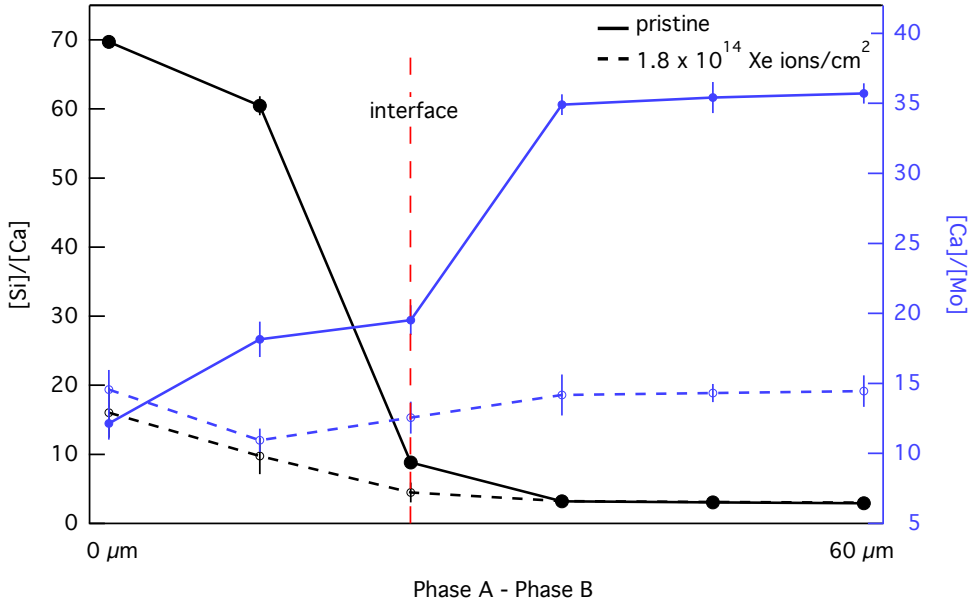

Figure S4. [Si]/[Ca] and [Ca]/[Mo] ratios from EDS analysis across the A – B interface of CM1 following Xe-irradiation with 1.8×10^{14} ions/cm^2. Trends indicate migration of Ca atoms from phase B to A, along with bulk-to-surface precipitation.

S3.0 XRD diffractogram

XRD was used to confirm that most of the compositions remained fully amorphous (even with multiple phases), before and after irradiation. This is easily identifiable from XRD data, as the spectra remain free of any diffraction peaks. There was one exception. In the main text, a single crystal was detected by diffraction for CM1 irradiated with 5×10^{12} ions/cm^2. The pattern in Figure S5 indicates a single crystal orientated along the [0 1 4] direction. The relative crystal content could not be accurately determined without powdering the sample and using an internal standard.

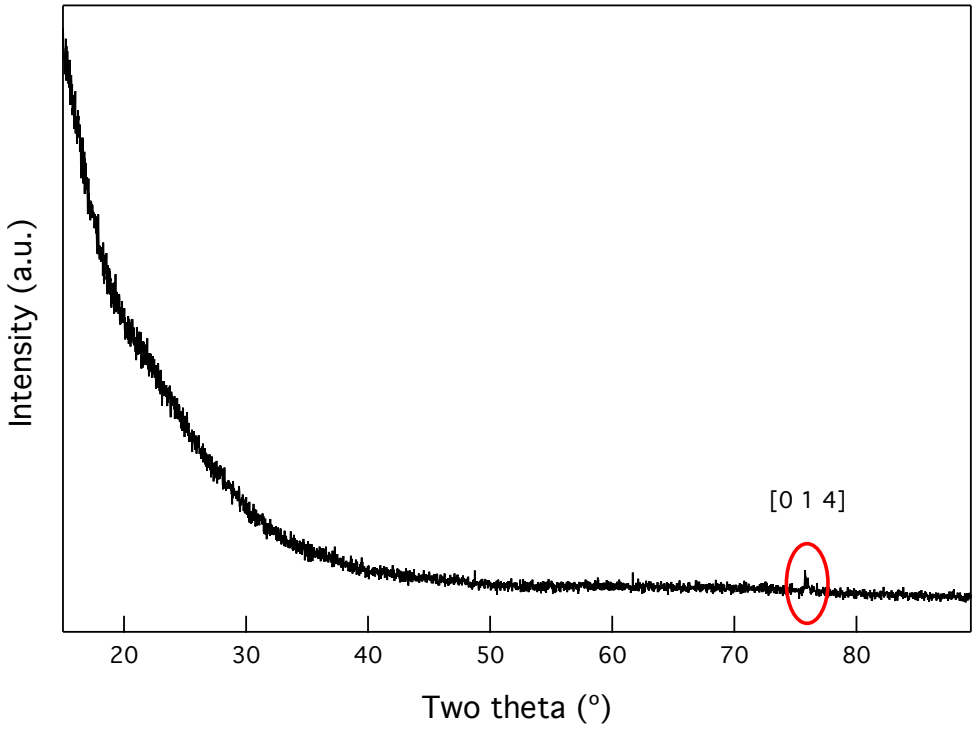

Figure S5: raw XRD spectra for CM1 irradiated with 5×10^{12} ions/cm^2. The single identifiable peak (circled) corresponds to [0 1 4] orientation.

S4.0 Additional Raman spectra of irradiated samples

Some of the Raman spectra for phase A in the CM series were provided in Figure 12, but those from phase B were qualitatively described, as there were several similar features in these spectra to those shown in Figure 9 of the main text. Figure S6 provides that Raman spectra for phases A and B in the calcium borosilicate glass without molybdenum. In this composition, the spectra for phase B show different structural features, with easily identifiable Q^n bands, where Q^n represents the Si-O stretching mode for SiO_4 tetrahedra with n bridging oxygen (850 - 1250 cm^{-1}). The spectra also show the presence of and rings containing one or two tetrahedrally coordinated boron units (700 – 800 cm^{-1}), B-O^- bond elongation, and danburite-like units (~ 630 cm^{-1}). Very few modifications are observed in these spectra for fluences between 1×10^{13} ions/cm^2 and 1.8×10^{14} ions/cm^2.

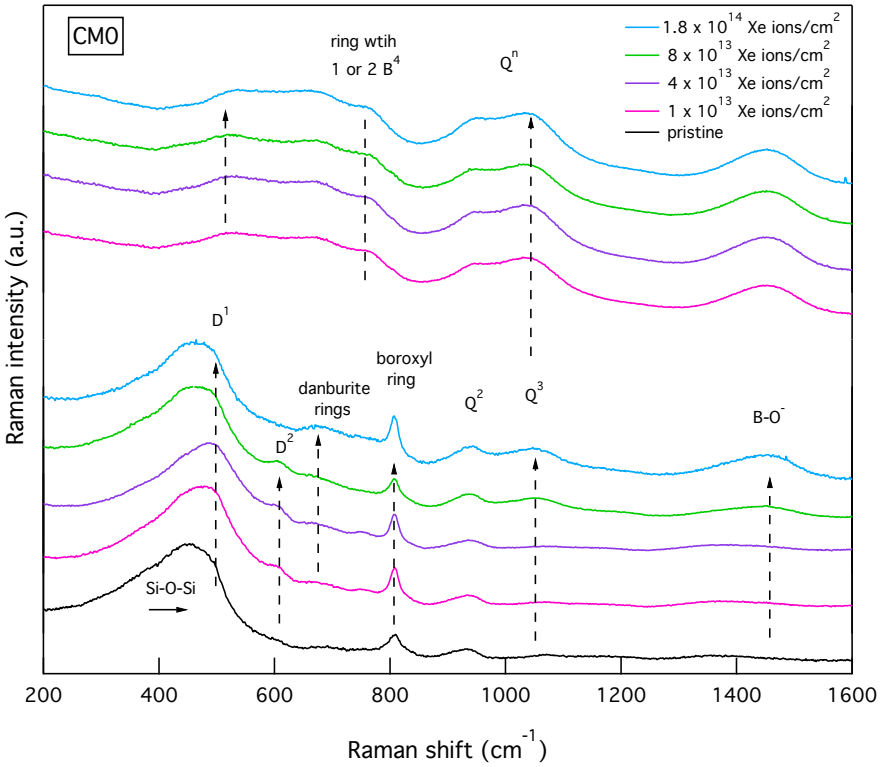

Figure S6: Raman spectra of two phases in CM0 following irradiation. The bottom five spectra are of phase A, while the top four are of phase B. Irradiation fluences are given in the legend, and bands of interest have been labeled.

The majority of trends in phase A are described in the main text, with an anomaly observed at the highest Xe fluence of 1.8×10^{14} ions/cm^2. At this dose, the intensity of the D^2 defect and area

of the *R* band appeared to decrease. This observation implies the initial formation (at low fluences), and subsequent cleavage of small SiO_4 rings with increasing Xe fluence, which is likely correlated to accumulating defects. Along with changes to Si-O bonding, there was also growth of the boroxyl ring and B-O^- bond elongation bands, which had reached a saturation between 4×10^{13} ions/cm^2 to 8×10^{13} ions/cm^2.

The Raman spectra for phases A and B in CM2.5 are provided in Figure S7. These spectra show that Xe-irradiation induced disorder that increased MoO_4^{2-} solubility and subsequently prevented the precipitation of molybdates, which was similarly seen in phase A. The Raman spectra of phase B in CM2.5 irradiated with 5×10^{12} ions/cm^2 to 1×10^{13} ions/cm^2 also showed a much larger *R* band contribution than samples with a dose greater than 1×10^{13} ions/cm^2 (see Figure S7). This result can be correlated to the proximity of the measured spot to phase C deposits with a spattered geometry. Using this theory, it can be predicted that phase C deposits are larger or have more significant edge spattering in samples irradiated with doses between 5×10^{12} ions/cm^2 to 1×10^{13} ions/cm^2. The micrographs in Figure 11 of the main text indicate that both size and distribution are likely contributors, as is an increased degree of mixing between phases B and C.

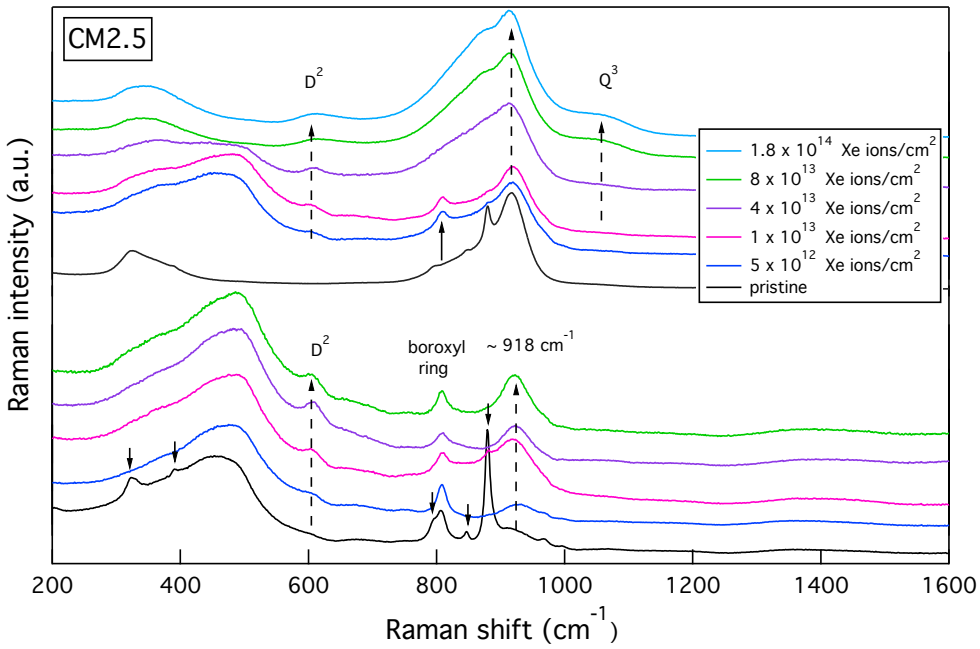

Figure S7: Raman spectra of phases A (Si-rich) and B (Mo-rich) in CM2.5 following Xe-irradiation. The bottom five spectra are of phase A, while the top six are of phase B. Irradiation fluences and bands of interest have been labeled.